

High-precision Mg abundances in the metal-rich Galactic disc: chemodynamical relations and comparison with chemical evolution models.

Santos-Peral, P.^{1,2}, Palla, M.^{3,4,5}, Recio-Blanco, A.², Kordopatis, G.², and and Fernández-Alvar, E.²

¹ Departamento de Física de la Tierra y Astrofísica, Universidad Complutense de Madrid, 28040 Madrid, Spain

² Université Côte d’Azur, Observatoire de la Côte d’Azur, CNRS, Laboratoire Lagrange, Bd de l’Observatoire, CS 34229, 06304 Nice cedex 4, France

³ INAF – Osservatorio Astronomico di Trieste, Via G.B. Tiepolo 11, 34131 Trieste, Italy

⁴ Dipartimento di Fisica, Sezione di Astronomia, Università di Trieste, Via G.B. Tiepolo 11, 34131 Trieste, Italy

⁵ Sterrenkundig Observatorium, Ghent University, Krijgslaan 281 - S9, 9000 Gent, Belgium

Abstract

The [Mg/Fe] abundance ratios are a fundamental fossil signature in Galactic archaeology for tracing the chemical evolution of disc stellar populations. High-precision chemical abundances, accurate stellar ages, distances, and dynamical data, together with their direct comparison with theoretical models, are crucial to infer the Milky Way formation history. We derived new more precise [Mg/Fe] abundances from the AMBRE:HARPS dataset, and estimated ages and dynamical properties using *Gaia* DR2 data. The data are compared with detailed chemical evolution models for the Milky Way, exploring different formation scenarios for the Galactic disc (i.e. the delayed two-infall and the parallel models). Our data favour the rapid formation of an early disc that settled in the inner regions, followed by the accretion of external metal-poor gas. The bulk of the data are well reproduced by the parallel and two-infall scenarios, but both scenarios have problems in explaining the most metal-rich and metal-poor tails of the low- α stars, which can be explained in light of radial migration from the inner and outer disc regions, respectively.

1 Introduction

This proceeding is a brief summary of the main results already published in the works from [1] and [2], we refer the reader to them for further detailed information.

The formation of the Galactic disc is still not well understood and in particular the origin and existence of a thin–thick disc bimodality is a matter of debate. The thick disc is often

reported to be $[\alpha/\text{Fe}]$ -enhanced relative to the thin disc, suggesting distinct chemical evolution histories, where the thick disc stellar population could have been formed on a short timescale before the epoch of the thin disc formation. In particular, magnesium is often used as an α -elements tracer. In a previous analysis ([3]), we showed a significant improvement in the precision of $[\text{Mg}/\text{Fe}]$ abundance estimates by carrying out an optimisation of the spectral normalisation procedure, in particular for the metal-rich population ($[\text{M}/\text{H}] > 0$), showing a decreasing trend in the $[\text{Mg}/\text{Fe}]$ abundance even at supersolar metallicities, partly solving the apparent discrepancies between the observed flat trend in the metal-rich disc (e.g. [4]), and the steeper slope predicted by chemical evolution models (e.g. [5]).

In this project, we use these new $[\text{Mg}/\text{Fe}]$ abundance measurements in order to study their impact on the observed chemodynamical features, and therefore on the interpretation of the Galactic disc evolution.

2 Data & Models

On the observational side, we considered the AMBRE:HARPS stellar sample ($R \sim 115\,000$, described in [6]), that corresponds to a total of 1066 stars in the solar neighbourhood, compiled from the analysed samples of [3] and [1]. The stellar $[\text{Mg}/\text{Fe}]$ abundances were derived by the spectrum synthesis algorithm GAUGUIN, following the described methodology in [3], where the spectral normalisation procedure was optimised for different stellar types with a significant improvement in precision. In addition, we estimated the orbital parameters with the *Gaia* DR2 astrometric positions and proper motions, and we also estimate the age for a subsample of main sequence turn-off (MSTO) stars using an isochrone fitting method (see [1] for details). Figure 1 illustrates the chemical distinction in the $[\text{Mg}/\text{Fe}]$ - $[\text{M}/\text{H}]$ plane for the stellar subsample with reliable age estimates, classifying the stars into high- and low- α population, commonly referred as the thick and the thin disc respectively.

On the theoretical side, we adopted two different chemical evolution scenarios to explain the chemical history of the solar annulus, assuming a 2 kpc ring centred at $R = 8$ kpc, also including prescriptions for stellar radial migration (see [2] for details):

1. Delayed two-infall model: MW forms by two sequential infall episodes. The first infall give rise to the high- α sequence, whereas the second (delayed and slower) infall forms the low- α stars. The second infall is delayed by 3.25 Gyr (see e.g. [5] [7]).
2. Parallel model ([8]): two separate infall episodes. Both evolve independently from different gas reservoirs, the infall episode forging high- α stars happens on shorter timescales than the one forming low- α ones.

In Figs 2 we show the predicted chemical evolution by the two proposed scenarios over the full observational dataset. Both models predict well the bulk of the stellar distribution in the $[\text{Mg}/\text{Fe}]$ versus $[\text{M}/\text{H}]$ plane. However, it can be seen that the two models do not explain the low- α , low-metallicity ($[\text{M}/\text{H}] \leq -0.6$ dex) data or the high-metallicity tail (above $[\text{M}/\text{H}] \sim 0.2$ dex) of the low- α sequence.

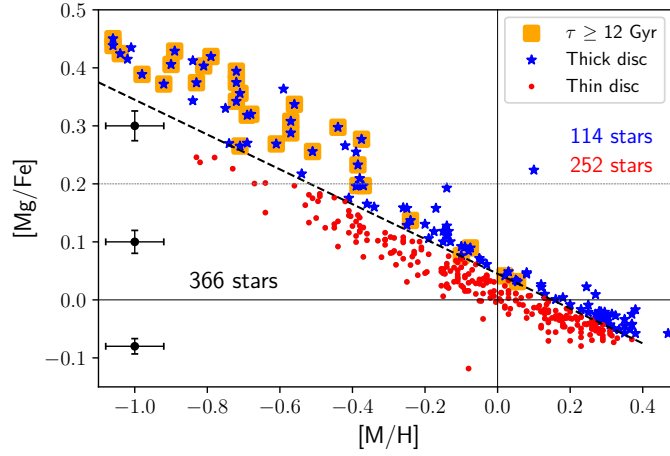


Figure 1: $[\text{Mg}/\text{Fe}]$ vs. $[\text{M}/\text{H}]$ for the stars with reliable age estimates. The stars with ages older than 12 Gyr are highlighted with orange squares. The black dashed line defines the thin (red circles)–thick (blue stars) disc chemical separation. The mean estimated errors are represented on the left-hand side for three different intervals in $[\text{Mg}/\text{Fe}]$.

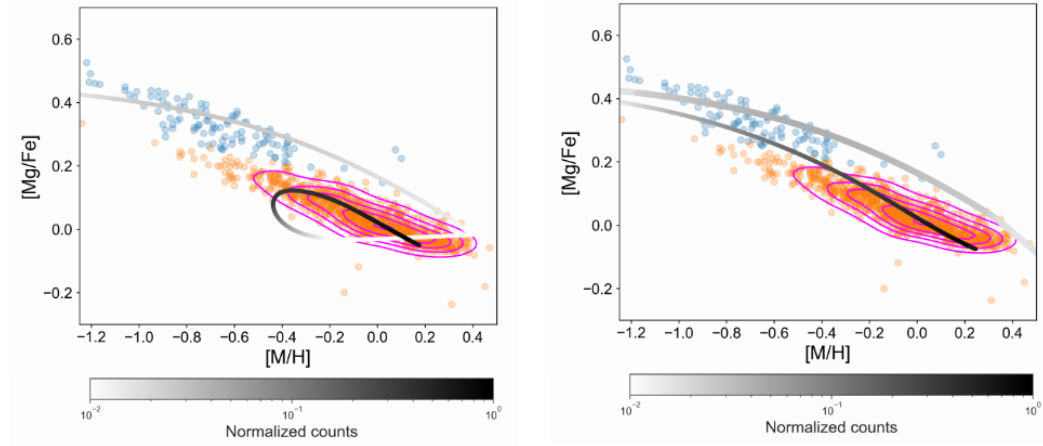


Figure 2: $[\text{Mg}/\text{Fe}]$ versus $[\text{M}/\text{H}]$ abundance diagram for the delayed two-infall (left panel) and the parallel (right panel) model scenarios of chemical evolution with [9] yields. The colour bar indicates the predicted stellar number counts. The light-blue points are the observed high- α stars, whereas the orange points are the observed low- α stars. The magenta contour lines enclose the observed density distribution of stars.

3 Temporal evolution in the $[\text{Mg}/\text{Fe}]$ - $[\text{M}/\text{H}]$ plane

We explored the distribution of $[\text{Mg}/\text{Fe}]$ and $[\text{M}/\text{H}]$ in the Galactic disc as a function of the Galactocentric position, and analysed the disc evolution with time.

Figure 3 illustrates the $[\text{Mg}/\text{Fe}]$ abundance ratios relative to $[\text{M}/\text{H}]$ for our MSTO stars,

in different age intervals and Galactic disc locations, assuming the guiding radius (R_g) as their true position in the Galaxy (top row: inner Galactic disc $R_g \leq 7.5$ kpc; bottom row: outer disc $R_g > 7.5$ kpc). We observe that the oldest stellar population ($\tau \geq 12$ Gyr) at every radius is located in what has been classically called the thick disc, that is, an α -enhanced population. During this early epoch, we observe rapid chemical enrichment, reaching solar metallicities. Interestingly, 11-12 Gyr ago, a second chemical sequence appears in the outer regions of the Galactic disc, populating the metal-poor low-[Mg/Fe] tail and starting at $[M/H] \sim -0.8$ dex and $[Mg/Fe] \sim 0.2$ dex. This corresponds to the population that has classically been referred to as the thin disc or low- α population, highlighted in the figure by red points. The average R_g of this second chemical sequence seems to be significantly larger than the Galactic disc extension at that time ($R_g < 8.5$ kpc), reaching the outer parts up to $R_g \sim 11$ kpc. Furthermore, those stars are shown to be significantly more metal-poor ($[M/H] \leq -0.4$ dex) with respect to the coexisting stellar population in the inner parts of the disc (top row). They also show lower [Mg/Fe] abundances than the older disc population in the outer parts (lower left panel), although presenting a similar metallicity distribution. This implies a chemical discontinuity in the disc around 11 Gyr ago, suggesting that the new sequence might have followed a different chemical evolution pathway from that followed by the previously formed component, possibly triggered by accretion of metal-poor external gas.

During the last 10 Gyr evolution (see [1]), we observe that the Galactic disc seems to have experienced a slower and more continuous chemical evolution towards more metal-rich and lower [Mg/Fe] regimes, without any remarkable star formation episode.

We performed a direct comparison with models to draw a more robust interpretation of our observational results:

Impact of inner and outer disc on the solar neighbourhood

The difficulties encountered by both the chemical evolution scenarios in predicting low- α , low metallicity and metal-rich stars (see Fig. 2) point towards a context where these stars were born at different Galactic locations from the solar vicinity. In this context, we did not consider the parallel scenario but rather the one-infall model that traces the formation of low- α sequence only.

In Fig. 4, we show the results of two-infall and one-infall models for outer ($R_g > 9$ kpc) and inner ($R_g < 7$ kpc) regions of the disc.

First, reproducing the outer Galactic regions (left-column panels), we need to adopt larger proportion of pristine gas during the second infall episode, reaching lower metallicities, to recover a good agreement with the two-infall model (top-left panel). On the other hand, the one-infall model for outer radii (bottom-left panel) naturally reproduce the tail of the low- α abundance trend for most of the data with large R_g (yellow crosses).

Secondly, regarding the inner parts of the Galaxy (right-column panels), the chemical tracks obtained with the two-infall model for inner radii (top-right panel) better reproduces the bulk of the metal-rich stars when a pre-enrichment (e.g. formation of the thick disc, Galactic halo, Galactic bar, previous merger event) in the second gas accretion episode is

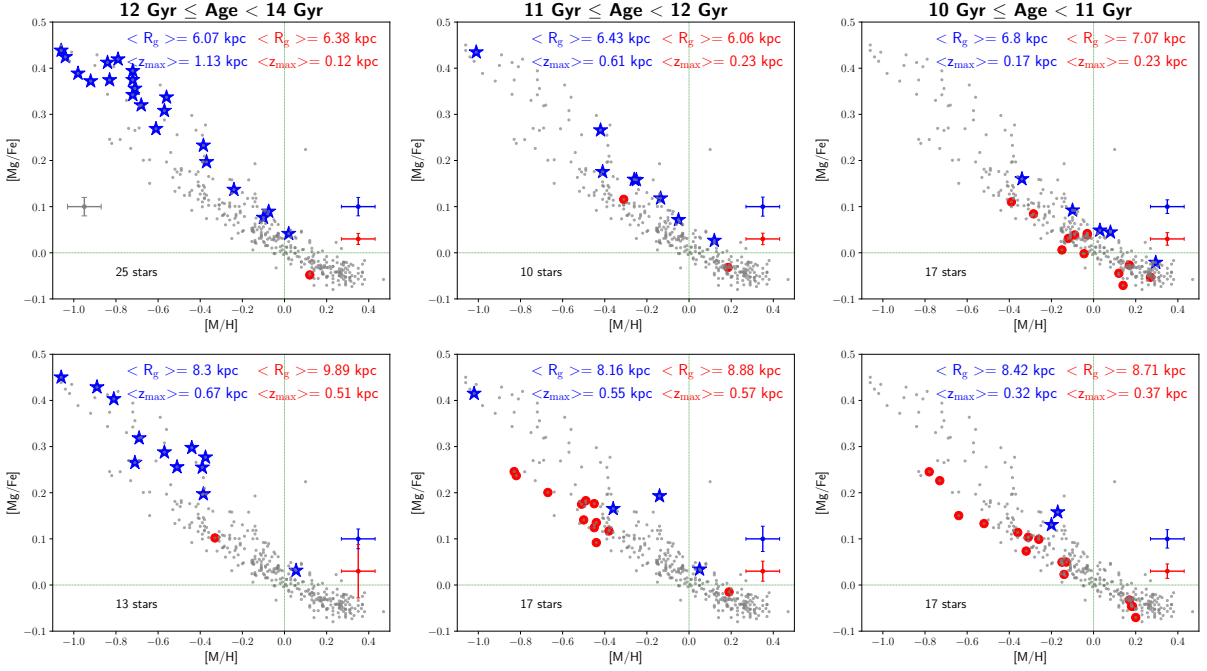


Figure 3: Distribution of the selected sample in the $([M/H], [Mg/Fe])$ plane at different ages and locations in the Galaxy (R_g). Two chemical sequences appear for ages younger than ~ 11 -12 Gyr, corresponding to the classical thick (blue stars) and thin (red circles) disc components. Each panel corresponds to a bin in the (age, R_g) space, dividing the Galactic disc into two regions: inner ($R_g \leq 7.5$ kpc; top row) and outer ($R_g > 7.5$ kpc; bottom row). The blue and red crosses in the bottom-right corner of each panel represent the mean estimated errors in $[Mg/Fe]$ and $[M/H]$ for the thick and thin disc population, respectively, at that particular radius and time. The average R_g and z_{max} for each population are given at the top of each panel. The whole MSTO sample is shown by the dotted grey points.

considered, enabling a larger rise in the $[\alpha/Fe]$ abundances. Contrary, we note that the one-infall model (bottom-right panel) has similar problems to the two-infall model without infall pre-enrichment, predicting lower $[Mg/Fe]$ abundances for a given metallicity.

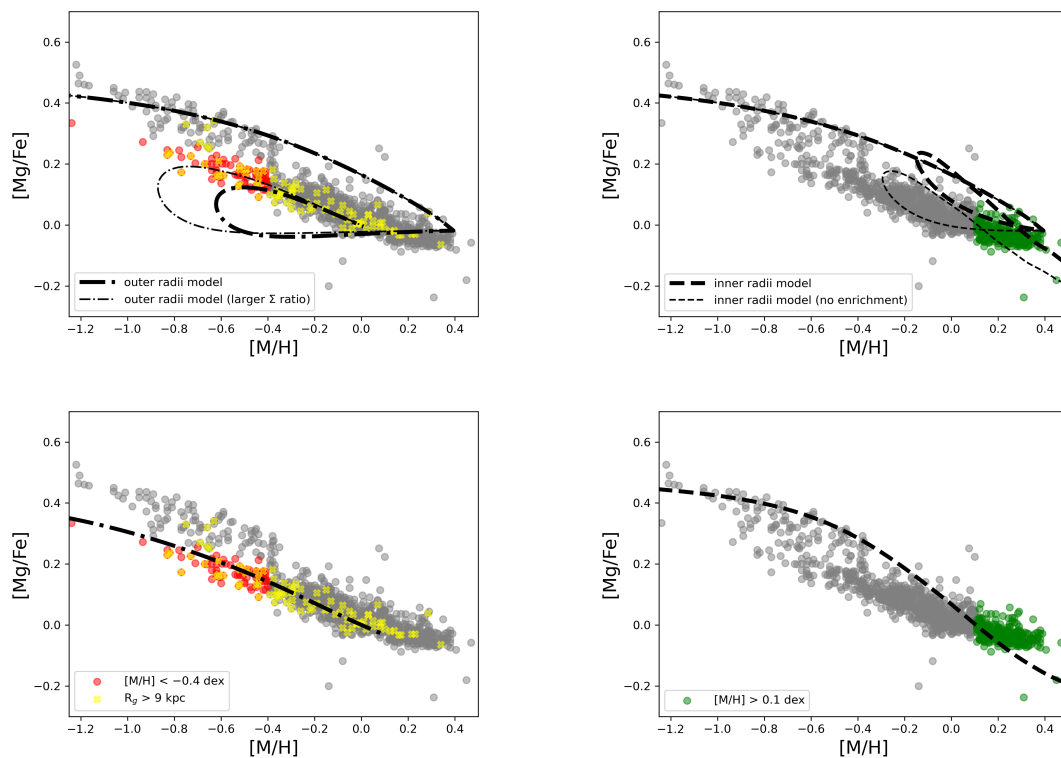


Figure 4: $[Mg/Fe]$ versus $[M/H]$ abundance diagram for the delayed two-infall (upper panels) and the one-infall (lower panels) models for outer ($R = 12$ kpc, dash-dotted lines, left panels) and inner Galactocentric radii ($R = 4$ kpc, dashed lines, right panels). The red points are the observed low- α , low metallicity stars ($[M/H] < -0.4$ dex), whereas the yellow crosses indicate the stars with guiding radius (R_g) larger than 9 kpc and the green points indicate the observed stars with $[M/H] > 0.1$ dex.

References

- [1] Santos-Peral, P., Recio-Blanco, A., Kordopatis, G., Fernández-Alvar, E., & de Laverny, P. 2021, *A&A*, 653, A85
- [2] Palla, M., Santos-Peral, P., Recio-Blanco, A., & Matteucci, F. 2022, *A&A*, 663, A125
- [3] Santos-Peral, P., Recio-Blanco, A., de Laverny, P., Fernández-Alvar, E., & Ordenovic, C. 2020, *A&A*, 639, A140
- [4] Hayden, M. R., Recio-Blanco, A., de Laverny, P., Mikolaitis, Š., & Worley, C. C. 2017, *A&A*, 608, L1
- [5] Palla, M., Matteucci, F., Calura, F., & Longo, F. 2020b, *ApJ*, 889, 4
- [6] De Pascale, M., Worley, C. C., de Laverny, P., et al. 2014, *A&A*, 570, A68
- [7] Spitoni, E., Verma, K., Silva Aguirre, V., et al. 2021, *A&A*, 647, A73
- [8] Grisoni, V., Spitoni, E., Matteucci, F., et al. 2017, *MNRAS*, 472, 3637
- [9] François, P., Matteucci, F., Cayrel, R., et al. 2004, *A&A*, 421, 613